

## 8

# Towards Routine Tensile Testing

T. Ohji

Government Industrial Research Institute, Nagoya,  
Hirate-cho, Kita-ku, Nagoya 462, Japan

### 1 INTRODUCTION

The tensile test is widely used in order to obtain information on the mechanical properties of commonly used industrial materials, because the testpiece is subjected to uniform stress so that measurements can be precisely and simply analysed. Therefore, tensile strength data are most important for the use of materials as structural components. However, in the case of ceramic materials, the high accuracy tensile test has been considered almost impossible to achieve because stress concentrations cannot be attenuated by plastic deformation due to its own brittle characteristics and consequently, even a very small eccentric load is liable to cause a large bending strain. Especially in high temperature measurements, the degree of difficulty is increased because the material and structure of testing devices are restricted.

The problems which stress concentrations bring about can be divided into two categories: fracture around grips and interference with a uniform stress distribution. An effective way to resolve both problems is to apply some sort of buffer material between testpiece and grip to relax stress; this method is used also for high temperature testing by holding the testpiece outside the furnace, for instance Lange *et al.* (1979). But from the viewpoint of economy, it is favourable to use a short specimen so that it is retained inside a furnace. For this purpose, the above problems should be dealt with only by optimising the geometries of the grip and testpiece to ensure that stress concentrations are not produced in the first instance since the grip is exposed to high temperature and a buffer material is not available. On this basis, in the tensile tests using commercially available hot-pressed silicon nitride and

sintered silicon carbide, the accuracy of the adopted testing method and the influence of specimen machining processes on fracture strength are described in addition to the high temperature tensile strength properties of the materials.

## 2 EXPERIMENTAL PROCEDURES

### 2.1 Tensile test assembly

The tensile test assembly for high temperature measurements in an air atmosphere used in this work is shown schematically in Fig. 1. The testpiece is retained by four SiC pins. As the testpiece is finished precisely and reproducibly in a profile cylindrical grinding machine, it is assured to be axially symmetrical. Accordingly, once the SiC pins are located accurately in the testpiece holder, the alignment of testpiece and holder can be assured. The holes in the SiC holders, as well as the universal joints and rods, were made within a tolerance of 0.01 mm by honing etc. The testpiece holder is linked to the rod with a universal joint. The SiC pins used in the universal joint are about 0.1 mm smaller in diameter than their holes. The clearance of 0.05 mm experimentally seems in the most suitable range for this case. The SiC rod is connected to a water cooling plate outside the furnace. Heat resistant bearings are used in order to absorb any torsional moment generated during the test because this connection is heated up to about 300°C when testing at 1300°C. The water cooled rods are fixed into a load cell or the frame of a testing machine through ordinary universal joints. An Instron 1185 is used for measurements in an air atmosphere.

In the furnace, a molybdenum disilicide heater is mounted so that it encloses almost the full area of the SiC tensile test jigs. The temperature variation along the gauge length area of the tensile test piece was measured using a Pt 10%Rh/Pt 30%Rh thermocouple and verified to be within 3°C.

An Instron 1125 machine was used for testing in a vacuum of  $10^{-4}$ ; a molybdenum mesh heater resulted in the temperature variation along the gauge length area being less than 3°C.

### 2.2 Tensile testpiece

Commercially available hot-pressed silicon nitride and pressureless sintered silicon carbide were used in this work. The tensile test specimens, whose geometry and dimensions are shown in Fig. 2, were fabricated from the billets as purchased. The plates (80 × 16 × 3 mm) cut from these billets were roughly ground by a 200 grit diamond wheel into the shape of Fig. 2,

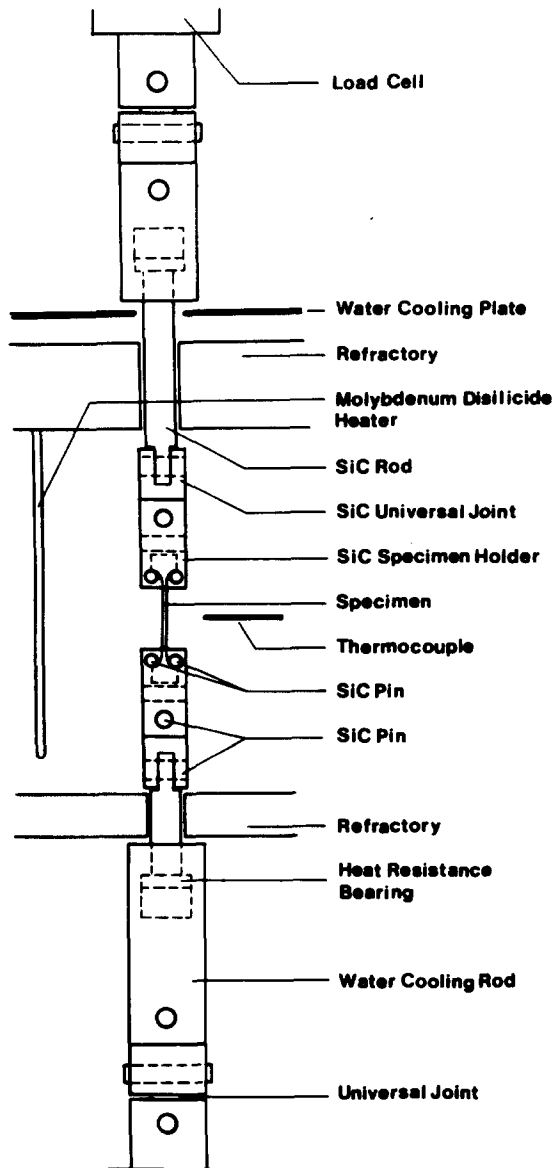


Fig. 1. Tensile test assembly for high temperature measurements.

and then finished by a 400 grit diamond wheel at a feed speed of 2 mm/min with a cutting depth of  $20\ \mu\text{m}$ . Finally, the gauge length area of each testpiece was hand polished along its length with 2000 grit diamond paste and a surface layer of several tens of micrometers was removed in order to eliminate the effects of residual stress and surface flaws produced in the machining process.

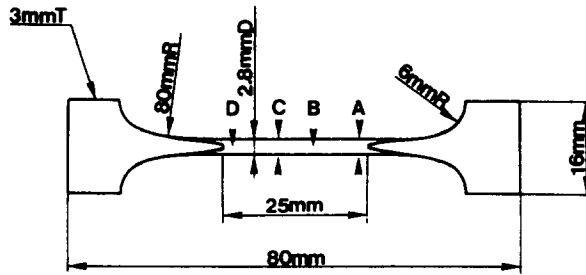


Fig. 2. Geometry and dimensions of tensile testpiece.

### 2.3 Miscellaneous test conditions

In this study, for the purpose of comparing tensile strength data, three point bending tests with a lower span of 30 mm were conducted with the use of rectangular bars of  $36 \times 4 \times 3$  mm which were cut from the same billets as the tension testpieces. All faces were finished lengthwise using 400 grit diamond wheels and edges were chamfered using 800 grit diamond whetstone.

The cross-head speed of 0.1 and 0.2 mm/min for tensile and bend testing respectively was selected so that the maximum strain rates were theoretically the same in both tests.

Both furnaces reached the test temperature in about 30 min and the testpiece was held at this temperature for 30 min to achieve thermal equilibrium before tests were started.

## 3 RESULTS AND DISCUSSION

### 3.1 Bending strains in tensile tests

In this tensile test method, fracture around the grips has been prevented by proper selection of the geometry and dimensions of the testpiece and holder. When testing hot-pressed silicon nitride, the specimen holders had SiC pins of 11-mm diameter, as shown in Fig. 3(a) and the specimen was in point contact with pins. In this holder, the contact positions are fixed, reproducible and axially symmetrical. As will be noted later, with this holder, the accuracy of tensile tests is very good, but the disadvantage is its high susceptibility to stress concentrations or fracture around grips. Accordingly this holder, although successfully used for silicon nitride, was not necessarily suitable for silicon carbide because the latter is more likely to have severe stress concentrations due to its high hardness and high elasticity. Figure 3(b) shows

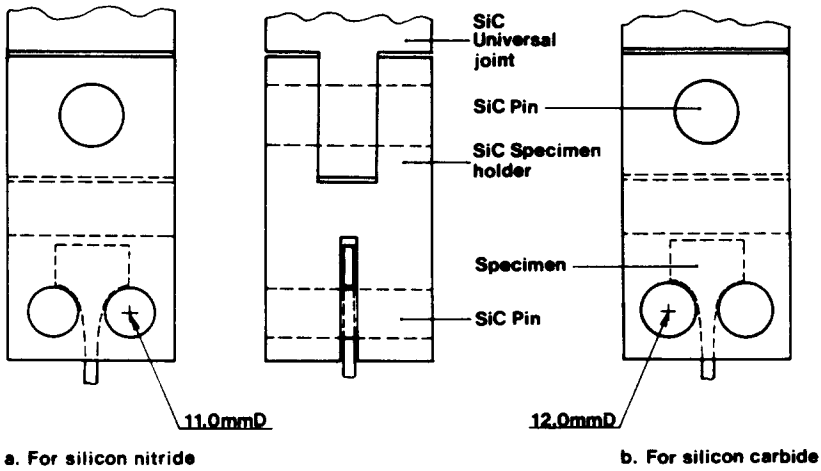


Fig. 3. Tensile testpiece holder for (a) silicon nitride; (b) silicon carbide.

schematically the specimen holder for silicon carbide. It has pins of 12-mm diameter so that the curvature of the testpiece holder conforms to the curved surface of the pins. For this case, the local stress concentration was thereby suppressed, but the contact position where load is transmitted, is not determinate and as a consequence, the accuracy is possibly lowered.

In order to investigate components of bending strains during room temperature tensile tests, strain gauges were attached at the positions indicated in Fig. 2 (for A and C both sides, and for B and D, front and rear).

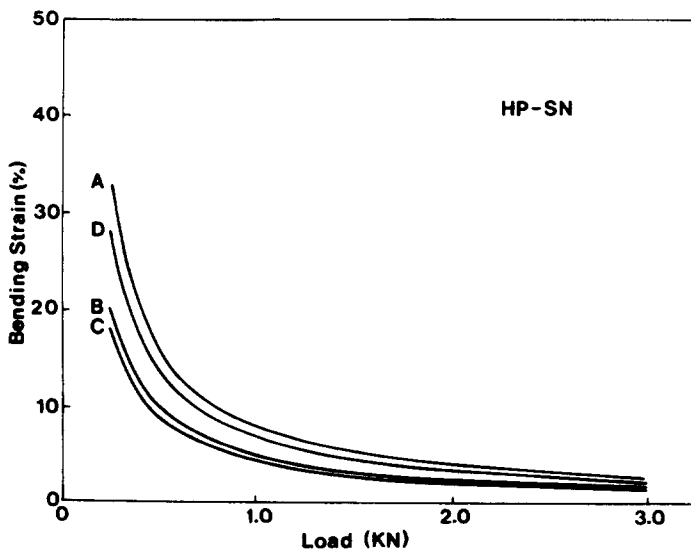


Fig. 4. Change of ratio of bending to tensile strain with load for hot-pressed silicon nitride.

Twenty-five measurements were made using hot-pressed silicon nitride and 20 using sintered silicon carbide. For all testpieces strain was measured at the positions B and C, and additionally for 10 of these, the measurements at A and D were also simultaneously recorded.

The change of mean value of bending strain with increasing load is described schematically in Figs 4 and 5 in the form of the ratio of bending to tensile strain. A common tendency was for the bending moment to be generated, at the instant of loading, but its magnitude remained unchanged whilst the load increased. As a consequence, the ratio is described by a hyperbolic function.

The bending strain detected at A and D, or near the ends of the gauge length area, tended to be larger than at B and C. One possible reason is that they are near the shoulder of the testpiece which is susceptible to localised stress concentration.

In high temperature measurements, before raising the temperature, axial alignment was such, at loads up to 500 N for silicon nitride and 1000 N for silicon carbide, that the bending strain on the surface was below 4% and 6%, respectively, of the tensile strain. After alignment, the lead wires of the strain gauges were cut and the furnace switched on. Whilst heating, a load of 5 N was constantly applied to the tensile test assembly to ensure that the axial alignment was not disturbed by heat expansion.

### **3.2 Recovery of tensile strength by removing surface layer**

The tensile test method may be evaluated from a knowledge of the ratio of internal fractures to the total, because the cross-section of the testpiece is subject to uniform stress and fracture occurs from the largest flaw within the gauge length area: this is likely to be within the bulk of the material. However, in a cylindrical grinder, the testpiece is ground perpendicularly to the tensile direction and the consequent machining flaws tend to be crucial to fracture. Additionally in the grinder, the small mutual eccentricity of testpiece and diamond wheel is liable to cause a severe defect. Accordingly, it is important to eliminate the influence of the machining process if a measurement of the proper strength is to be made: this is particularly so when using small testpieces, as in these experiments.

For the purpose of identifying the influence of the machining process, three types of testpiece were made. The first was tested 'as-machined'; the second had 25  $\mu\text{m}$  removed by hand polishing before testing, and the third had 50  $\mu\text{m}$  removed. The recovery of fracture strengths and the reduction of the surface fracture ratio with increasing depth of surface removal is shown in Table 1 for both materials.

As the common tendency, 25  $\mu\text{m}$  surface removal gives rise to a

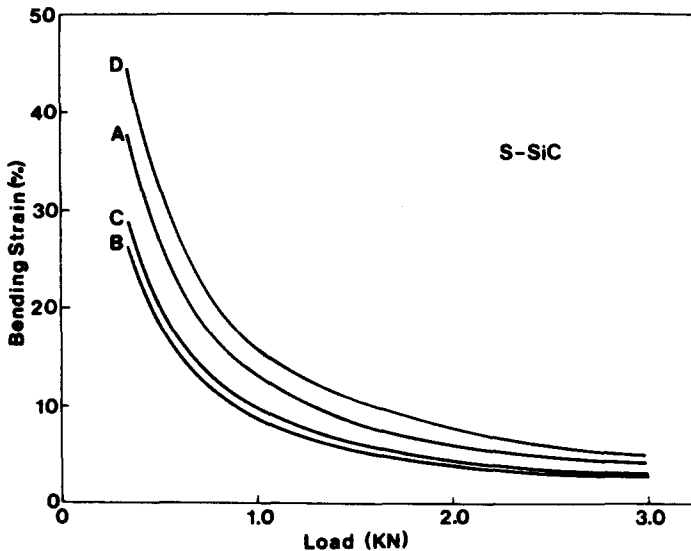


Fig. 5. Change of ratio of bending to tensile strain with load for sintered silicon carbide.

remarkable improvement of fracture strength with a corresponding increase in the fraction undergoing internal fracture, and lets the measured strength approach the inherent one. Most of the increase in strength can be attributed to the large recovery of surface fracture strengths. More than 30% and 60% increases are attained after 25  $\mu\text{m}$  surface removal for silicon nitride and silicon carbide respectively, and they reach almost the same level as internal fractures which also show little increase with surface removal. It is considered that the surface fracture of an 'as-machined' testpiece occurs at machining flaws generated in cylindrical grinding, whilst fracture is mostly initiated from inherent surface flaws in testpieces which have received the hand-polishing.

In the hand-polished process, one should ensure that the surface has been removed uniformly over the full gauge length area. 'Ordinary' or careless hand-polishing has the tendency to concentrate on the central regions of the gauge length area and to leave both end portions where bending strains are greatest (see Figs 4 and 5).

### 3.3 Tensile strength properties of hot-pressed silicon nitride

#### 3.3.1 High temperature strength distribution

The tensile strengths of 25 testpieces of hot-pressed silicon nitride were measured at both room temperature and 1200°C in a vacuum atmosphere. Bending tests were also conducted at both temperatures. This material was

**TABLE 1**  
Recovery of Strength by Removing Damaged Surface

<i>Depth of lapping (<math>\mu\text{m}</math>)</i>	0	25	50
<i>(a) Hot-pressed silicon nitride</i>			
Sample size	10	10	25
Ratio of internal fracture (%)	40	70	84
Overall strength (MPa)	608 (95)	755 (102)	768 (105)
Internal fracture (MPa)	685 (118)	725 (92)	752 (113)
Surface fracture (MPa)	556 (71)	785 (68)	794 (83)
<i>(b) Sintered silicon carbide</i>			
Sample size	10	10	20
Ratio of internal fracture (%)	20	60	70
Overall strength (MPa)	325 (55)	510 (108)	505 (86)
Internal fracture (MPa)	385 (81)	515 (90)	477 (85)
Surface fracture (MPa)	315 (40)	507 (102)	556 (70)

( ) = standard deviation.

sintered with 5 weight % yttria and 3 weight % alumina and contained (in weight%) 0.014 Mg, 0.013 Cr, 0.022 Fe and 0.024 Ca as impurities. The density was 3.199 Mg/m<sup>3</sup>.

At room temperature, the Weibull modulus and mean strength resulted in 8.6 and 765 MPa for tension and 14.2 and 1030 MPa for bending, which is a large difference. The theoretical tensile strength estimated from bending strength and its modulus is 671 MPa, which is much lower than the experimental value, 765 MPa. However, at the high temperature of 1200°C, the Weibull moduli are increased to 20.0 for tension and 25.7 for bending, although strengths are lowered as shown in Fig. 6. The improvement of the Weibull modulus in the tensile test is remarkable. The theoretical tensile strength is calculated to be 399 MPa from the bending strength and has a good agreement with the experimentally measured value of 377 MPa. The fracture strength distribution of hot-pressed silicon nitride at 1200°C seems to be represented by one Weibull distribution.



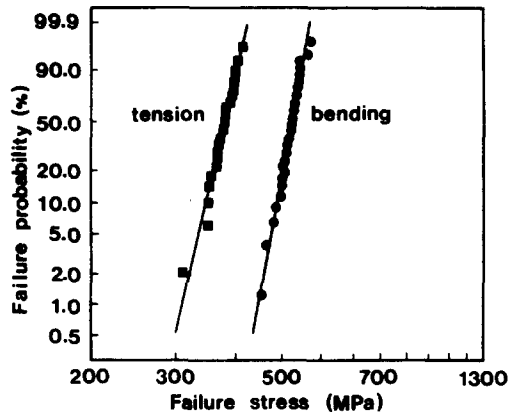


Fig. 6. Weibull plots of tensile and bending strength for hot-pressed silicon nitride at 1200°C.

The change of mechanical properties with temperature is attributed to the presence of a glassy phase at the grain boundaries. A TEM image of the hot-pressed silicon nitride used in this experiment is shown in Fig. 7. It is known that the silicon nitride grain is fully surrounded by glassy phase indicated by G1. With increasing temperature, the viscosity of the glassy phase is reduced and, along with the decreasing mechanical strength, the plastic region around the tip of a crack is expanded and the fracture mechanics which are valid at room temperature become inapplicable. That is to say, the crack size

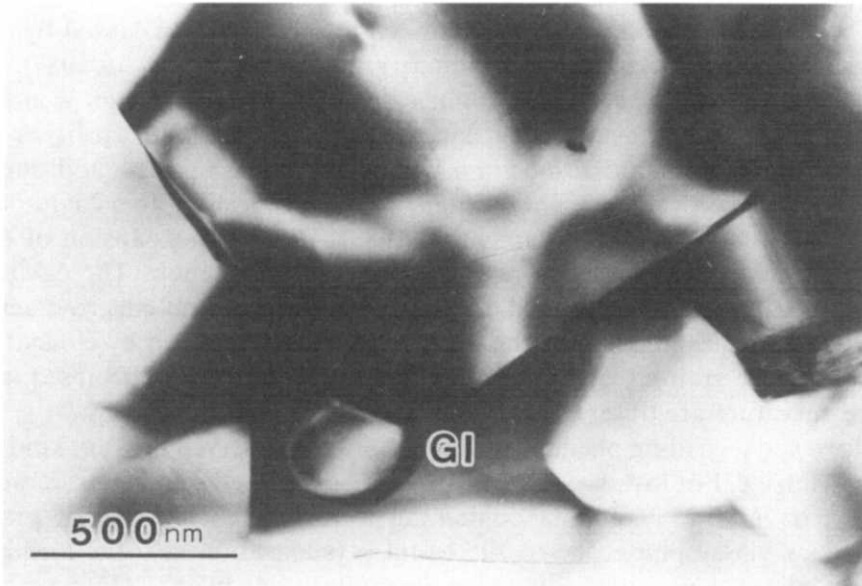


Fig. 7. Silicon nitride grain and glassy phase (G1).

dependence on strength where fracture strength is inversely proportional to the square root of crack size may be decreased at elevated temperatures.

### 3.3.2 Yielding phenomena

At temperatures higher than 1200°C, the failure of silicon nitride is accelerated by cavity nucleation and propagation associated with viscous hole growth and, therefore, shows more complicated characteristics than the brittle fracture at lower temperatures. Consequently, the stress/displacement relationship in mechanical strength tests exhibit non-elastic behaviour. The failure mechanism associated with cavity nucleation and propagation was investigated.

Changes in stress/displacement diagrams at intervals of 20°C are shown in Fig. 8, where stress is the load divided by the original cross-section area of the testpiece (engineering stress). The displacement shown in Fig. 8 is the distance moved by the cross-head of the testing device, which includes the elongation of the device itself as well as the shoulders of the testpiece. At 1300°C the stress falls, showing a peak (upper yielding point) before fracture. At temperatures above 1320°C, the stress rises again through the transitional region (lower yielding point) following the decrease, and then describes a large curvature until fracture. In the range from 1340 to 1380°C, fractures occur when the stress reaches the maximum point, while above 1400°C a small decrease in stress from that point was measured before fracture. The fractured testpieces did not show any localised extension, but uniform extension of the gauge length area was obtained.

The yielding phenomena were attributed to the cavitation caused by the decreased viscosity of the grain boundary glassy phase (Ohji *et al.*, 1987). As the load increases, the cavities first nucleate at triple points and grow along grain boundaries, resulting in large scale cavities. This process is accompanied by the adjacent grain boundary sliding and the additional cavity nucleation at the neighbouring triple points, leading to a cavitation zone formation (Evans & Blumenthal, 1983). The rapid expansion of the cavitation zone produces the upper yielding phenomenon. The cavities produced in this process tend to link together to form macro-cracks. However, the propagation of the macro-cracks is obstructed by elongated silicon nitride grains. Consequently, a lower yielding point and subsequent large curvature are observed in the stress/displacement diagrams.

However, a yielding phenomenon is not always observed in every kind of silicon nitride. For instance, a tensile test on hot-pressed silicon nitride with 4% yttria and 2% alumina containing a very small amount of grain boundary glassy phase due to successful crystallisation into the mullite phase did not show any yielding phenomenon even at 1450°C. On the other hand, pressureless sintered silicon nitride with 12% alumina and 6% yttria

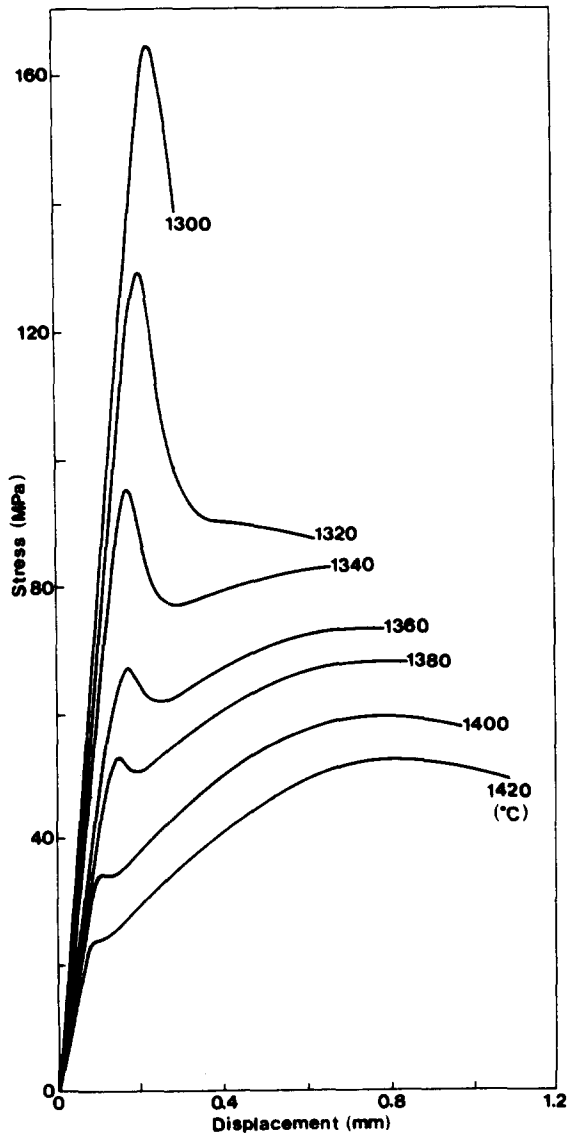


Fig. 8. Stress/displacement diagrams of hot-pressed silicon nitride as a function of temperature.

containing 0.2% calcium impurity, which is considered to contain a more glassy phase of lower viscosity (Kossowsky *et al.*, 1975), started a similar yielding phenomenon at 1240°C.

### 3.4 Tensile strength properties of sintered silicon carbide

Commercially available silicon carbide sintered with about 0.5 weight% boron carbide and 2 to 3 weight% carbon was used in this experiment. The

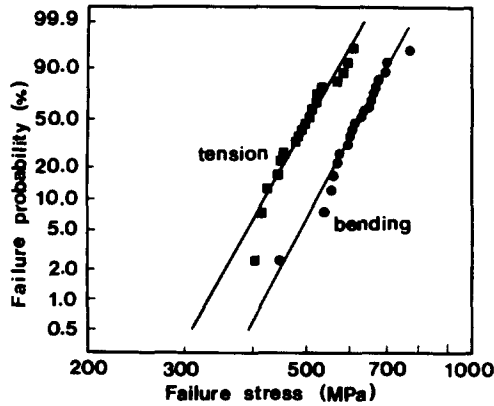


Fig. 9. Weibull plots of tensile and bending strength of sintered silicon carbide at 1300°C.

density was 3.12 Mg/m<sup>3</sup> and 0.040 Al, 0.004 Mg, 0.015 Cr, 0.197 Fe and 0.030 Ca (in weight%) were contained as impurities.

Tensile and bending distributions at room temperature and 1300°C were measured using 20 testpieces for each (Fig. 9). The Weibull moduli and mean failure strengths at room temperature were, respectively, 12.0 and 505 MPa for tension and 9.0 and 671 MPa for bending. At 1300°C, the equivalent results were 10.7 and 512 MPa for tension and 11.5 and 651 MPa for bending. Although the quantity of testpieces may not be adequate to obtain a precise Weibull modulus for each distribution, it is ranging from 9 through 12, showing rather good agreement with one another. However, the theoretical tensile strength calculated from bending strength and its Weibull modulus was 412 and 426 MPa at room temperature and 1300°C, respectively, and was lower than the actually measured strength for both temperatures. This discrepancy may be attributed to the presence of flaws

TABLE 2  
Types of Fracture Defects

	Ratio (%)	Mean St. (MPa)	Size (μm)
Surface flaw	35	556	—
	45	564	—
Pore	65	477	40–80
	45	460	40–85
Bridge cavity	0	—	—
	10	512	40–50

Top figure: R. T., bottom figure: 1300°C.

and residual stresses on the surface of bending testpieces after the machining process.

Fractography by use of an optical microscope and SEM showed that the fracture origins of almost half of the tensile testpieces were located on the surface irrespective of temperature. The types of fracture defects could be divided roughly into three categories as shown in Table 2. Most of the

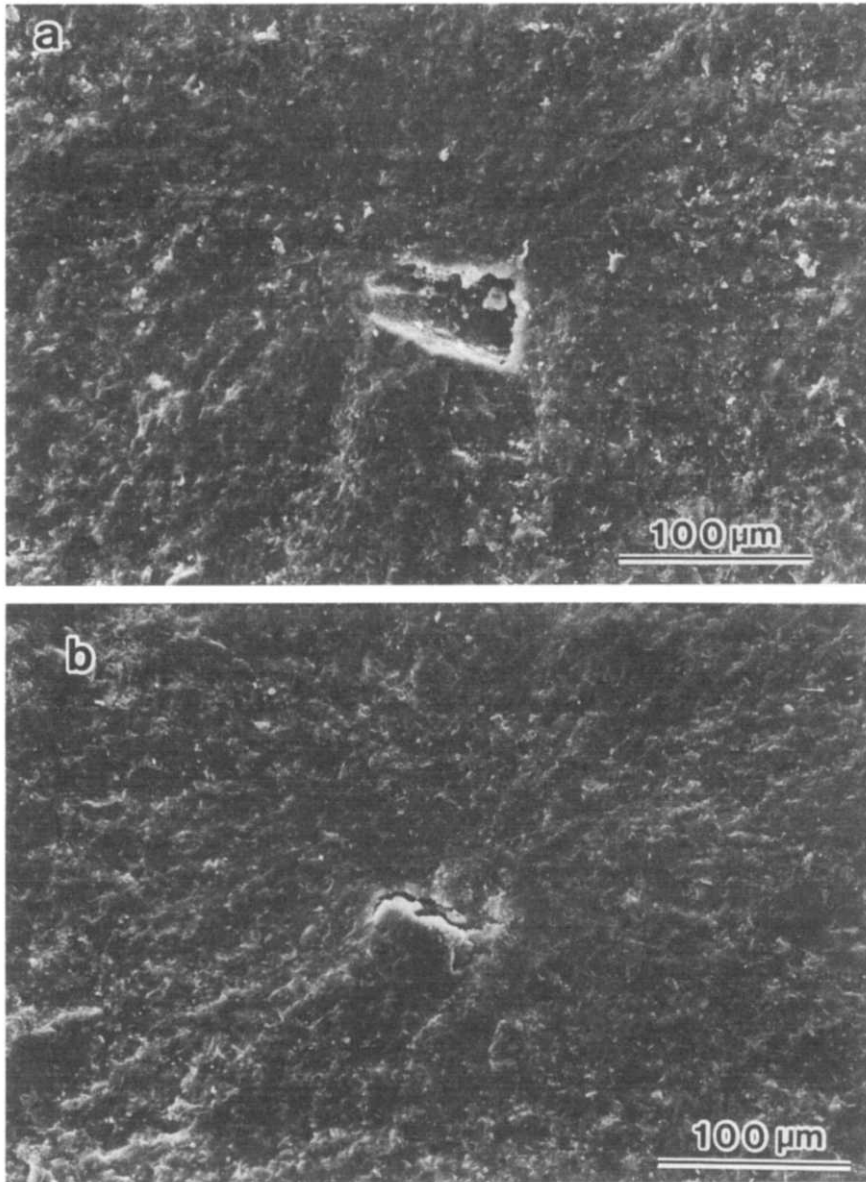


**Fig. 10.** Typical examples of (a) pore; (b) bridging cavity.

fractures from surface flaws originated at the ends of the gauge length area, suggesting some influence of stress concentration. Testpieces fractured with a low strength tended to have internal fracture origins, and most of them were thought to have originated at a kind of pore. A typical example of a pore is shown in Fig. 10(a). The most likely process by which this kind of pore is produced is from a rather coarse foreign matter introduced in the handling of the powder. By agglomerating with fluoro-resin powder particles, used as a lubricant in moulding, it remains as a large void in the sintered body (Suzuki, 1984). Two specimens were shown to fail at 1300°C from what are called bridging cavities: one of them is shown in Fig. 10(b). It is considered that, if the fluidity of the powder is poor, a scatter in green moulding density of induced and defects originating in or associated with bridging in the green moulding are generated.

The accuracy of the tensile tests using silicon carbide is not excellent, as noted in Fig. 5, but still the internal fractures occupied 65% of the total at room temperature and 55% at 1300°C. It appears that the influence of low accuracy or the additional stress from bending on the data is apparently small, probably because the scatter of stress distribution is absorbed by the variation of properties in the material itself.

#### 4 CONCLUSIONS

A tensile testing method for high temperature measurements has been proposed and its accuracy assessed by measuring the influence of the testpiece machining process on fracture strength. The testing method deals with two problems caused by stress concentration—the fracture around grips and the variation in stress distribution—by optimising the geometries of the grip and testpiece so as not to initiate a stress concentration. Particularly for silicon carbide, the curvature of the pins holding the testpiece was selected to follow the shoulder of testpiece in order to prevent the initiation of fracture. In a tensile test, a bending moment is generated once the loading starts, but is almost unchanged whilst the load increases. Therefore the ratio of bending to tensile strain is described by a hyperbolic function. The influence of the machining process on fracture strength is of great importance and should be eliminated to obtain proper results. As an illustration, a 25- $\mu\text{m}$  surface removal by hand-polishing gave rise to a remarkable improvement of fracture strength and a corresponding increase in the number of internal fractures; furthermore, the measured strength approaches the inherent one. Most increases in strength can be attributed to the large recovery of surface fracture strength.

The tensile tests on silicon nitride and silicon carbide were conducted

using the above testing method. The mechanical strength of silicon nitride in both tension and bending is degraded at 1200°C due to the presence of glassy phases at grain boundaries, but the Weibull modulus increased, particularly in tensile strength as the plastic region around the tip of a crack expanded and the crack size dependence on strength may be decreased at elevated temperatures.

At temperatures higher than 1200°C, the failure of silicon nitride is accelerated by the cavity nucleation and propagation associated with viscous hole growth and, therefore, shows more complicated characteristics than the brittle fractures at lower temperatures. Consequently, the stress/displacement relationships in mechanical strength tests exhibit a non-elastic behaviour or a yielding phenomenon.

Tensile and bending strength distributions of silicon carbide at room temperature and 1300°C resulted in Weibull moduli ranging from 9 to 12, showing rather good agreement with one another. The fracture defects observed in SEM were divided into three types: surface flaw, pore and bridging cavity. Most of the internal fractures originated from pores which were caused by the inclusion of foreign matter during processing.

## REFERENCES

- Evans, A. G. & Blumenthal, W. (1983). High temperature failure in ceramics. In *Fracture Mechanics of Ceramics*, Vol. 6, Plenum Press, New York, pp. 423–48.
- Kossowsky, R., Miller, D. G. & Diaz, E. S. (1975). Tensile and creep strengths of hot-pressed silicon nitride, *J. Mater. Sci.*, **10**, 983–97.
- Lange, F. F., Diaz, E. S. & Anderson, C. A. (1979). Tensile creep testing of improved Si<sub>3</sub>N<sub>4</sub>. *Am. Ceram. Soc. Bull.*, **58**(9), 845–8.
- Ohji, T., Sakai, S., Ito, M., Yamauchi, Y., Kanematsu, W. & Ito, S. (1987). Yielding phenomena of hot-pressed silicon nitride. *High Temperature Technology*, **15**(3), 139–44.
- Suzuki, H. (1984). Material design in structural ceramics, *Bull. Ceram. Soc. Jap.*, **19**(5), 411–14.